Escobar-Sierra, Diana Marcela; Stiven Posada-Carvajal, Johnnatan; León Atehortúa-Soto, Diego
Fabrication of chitosan/bioactive glass composite scaffolds for medical applications

Fabrication of chitosan/bioactive glass composite scaffolds for medical applications

Fabricación de andamios compuestos de quitosano y vidrio bioactivo para aplicaciones médicas

Diana Marcela Escobar-Sierra*, Johnnatan Stiven Posada-Carvajal, Diego León Atehortúa-Soto

Grupo de Investigación en Biomateriales, Facultad de Ingeniería, Universidad de Antioquia UdeA, Calle 70Nº 52-21, Medellín, Colombia

ABSTRACT: In the current study, a bioactive glass (BG) powder was prepared by sol-gel technique in the system SiO_2–CaO–P_2O_5, and both, bioactive glass precursors (BGi) and the powder of bioactive glass (BGp) were used to produce crosslinked chitosan composite scaffolds (CH/BGi and CH/BGp), which were produced by lyophilization. The bioactive glass was analyzed to know its composition, crystallinity and morphology through Raman Spectroscopy (RS), X-Ray Diffraction (XRD) and Scanning Electron Microscopy (SEM), respectively. In addition, compression strength tests were carried out on the resulting composite scaffolds. Experimental results show that the fabricated CH/BG scaffolds might be a promising composite biomaterial for bone tissue engineering, due to the XRD results, showing a pollutant-free biomaterial, and, SEM shows bioactive glass particles homogenously distributed within the chitosan matrix which suggested that the developed composite scaffolds possess the prerequisites for tissue engineering and these can be used for tissue engineering applications.

RESUMEN: En el presente estudio, un polvo de vidrio bioactivo (VB) fue preparado por la técnica sol-gel en el sistema SiO_2-CaO-P_2O_5, y ambos, precursores de vidrio bioactivo (VBi) y polvo de vidrio bioactivo (VBp) se utilizaron para producir andamios compuestos por quitosano y vidrio bioactivo (Qno/VBi y Qno/VBp), los cuales fueron producidos por liofilización. El vidrio bioactivo fue analizado para conocer su composición, cristalinidad y morfología a través de Espectroscopía Raman (RS), Difracción de Rayos X (DRX) y Microscopía Electrónica de Barrido (MEB), respectivamente. Además, pruebas de resistencia a la compresión se llevaron a cabo sobre los andamios compuestos resultantes. Los resultados experimentales muestran que los andamios de Qno/VB podrían ser un biomaterial compuesto muy prometedor para ingeniería de tejido óseo, debido a los resultados de DRX, que muestra un biomaterial libre de contaminantes, además el SEM muestra partículas de vidrio bioactivo homogéneamente distribuidas dentro de la matriz de quitosano sugiriendo que los andamios de material compuesto desarrollados poseen los requisitos previos para la ingeniería de tejidos y que éstos pueden ser utilizados para aplicaciones de ingeniería de tejidos.

1. Introduction

Recently, tissue engineering has been extensively investigated as a promising approach for tissue regeneration, to replace or repair tissues in the human body, when a significant loss of tissue occurs as result of trauma, accident or deformation.

Treatments that employ graft material retrieved from a different site in the patient's body (autograft), from another human donor (homograft), or from other species (heterograft) are restricted by their limited availability, complications and the risk of disease transmission [1].

In order to face this situation, biomaterials have been used for the production of three-dimensional (3D) structures, denominated scaffolds, which provide more advantages than powder, granulated materials or even some of the before mentioned transplants. These scaffolds have the potential to induce bone regeneration and are able to degrade after a certain period after implantation [2-4]. The achievement of stable direct contact between bone and the scaffold surface is a critical requirement for the development of optimal scaffolds and such surface contact must be structural, mechanical and functional. In addition, non-toxicity, biocompatibility and an adequate mechanical strength are necessary to obtain suitable scaffolds for implantation.

The scaffold's microstructure could range from membranes to porous structures. Also for their fabrication, several biodegradable materials (synthetic polymers as polycaprolactone, polylactic-co-glycolic acid, polyethylene

glycol, polyvinyl alcohol and natural polymers as alginate, collagen, gelatin, chitin, chitosan) [5, 6] and ceramics (hydroxyapatite and bioactive glasses) have been explored and the possibility of processing hybrid polymer/ceramics scaffolds have gained considerable attention for improving mechanical properties and biodegradation on tissue engineering applications [7, 8].

Among natural polymers, chitin is widely used because it is a natural polysaccharide found in the shell of several crustaceans, cuticles of insects and cell walls of fungi. Chitosan, as chitin derivate, is obtained by partial deacetylation (at least about 50%) under generally alkaline conditions [9].

Chitin as polymer, has been proved to be biocompatible, biodegradable, non-antigenic, non-toxic and biofunctional. It exhibits antimicrobial activity, for which has been popularly used on agriculture [5] and the medical field for several applications, including wound dressings, drug carriers and scaffolds for tissue engineering [10]. In addition, properties of chitosan scaffold, such as microstructure, crystallinity and mechanical strength, can be modulated by changing chitosan concentration, freezing rate, as well as the molecular weight and percent of deacetylation of chitosan.

Among bioactive ceramics, bioactive glasses have gained importance for biomedical devices because they are biocompatible, bioactive, osteoconductive and osteoinductive, due to their ability to generate the apatite layer on the surface, which is chemically tied with bone when implanted in the human body [3, 11, 12].

Some recent studies show that the processing of chitosan/bioactive glass composites improves the mechanical and biological properties. Chitosan favors cell adhesion due to its chemical nature and bioactive glass particles provides biomineralization and it increases the stiffness of polymer material without decrease the mechanical strength [13, 14].

Hence, considering the physical, chemical and biological properties of these biomaterials, it is interesting to research the possibility of preparing scaffolds using a chitosan matrix reinforced with bioactive glass to evaluate the influence of the ceramic addition on the scaffold's properties used on tissue engineering [6, 15].

Based on these assumptions, in this paper the preparation of bioactive glass by sol-gel is addressed and also a processing technique to obtain hybrid chitosan/bioglass scaffolds for tissue engineering is presented, using the sol-gel-derived bioactive glasses (both powder and precursors in solution) and chitosan solution as pattern sample. Then, chitosan/bioactive glasses (CH/BG) composite scaffolds were characterized by several techniques. In the end, analysis and conclusions are presented.

The aim of this study was to prepare CH/BG composite scaffolds with BG in different states (solution of precursors and powder), using two different methods proposed by [10, 16]. One with BG precursors and the other with BG powder,

coupled with chitosan. The microstructure was evaluated by spectroscopy, microscopy techniques, and compression tests to observe the best method and the best ratio of chitosan/hydroxyapatite to obtain scaffolds with more adequate properties to be used in tissue engineering.

2. Materials and methods

This study presents a simple but efficient method to prepare CH/BG composite scaffolds with a porous structure. This technique involved the preparation of precursors, co-precipitation, molding, and consequent freeze-drying.

2.1. Preparation of solutions

Tetra-Ethyl-Ortho-Silicate (TEOS, Merck) was added to a solution 1N of Nitric Acid (HNO_3, Carlo Erba Reagent). Then, Calcium Nitrate tetrahydrate ($Ca(NO_3)_2.4H_2O$, PRS Panreac) and Phosphorus Pentoxide (P_2O_5, PRS Panreac) were added as precursors to synthesize bioactive glass sol. To raise the pH of the bioactive glass sol-gel, a Sodium Hydroxide (NaOH, Merck) 5% p/v solution was added in the resultant solution.

For the scaffolds matrix preparation, Chitosan obtained from shrimp (Sigma Aldrich, >75% deacetylation) was used and diluted on a solution of Glacial Acetic Acid ($C_2H_4O_2$, PRS Panreac). As crosslinking agents for polymeric matrix formation, Polyvinyl alcohol (PVA Sigma Aldrich 13000-23000 Dalton molecular weight and 98% hydrolysis) and Tripolyphosphate (TPP) were used.

2.2. Production of bioactive glass (BG)

The bioactive glass was prepared by sol-gel technique with an average ratio of 65% SiO_2, 5% P_2O_5 and 30% CaO, for which TEOS ($C_8H_{20}O_4Si$ Merck), HNO_3 (Carlo Erba), P_2O_5 (Panreac PRS) and $Ca(NO_3)_2.4H_2O$ (Panreac PRS) were mixed as defined below: 0.065 mol of TEOS was added into 20 mL of 0.1M nitric acid (HNO_3) the mixture was allowed to react for 30 minutes to promote the acid hydrolysis of TEOS. Then, 0.05 mol of P_2O_5 was added and mixed during 45 minutes, and finally, 0.03 mol of $Ca(NO_3)_2.4H_2O$ was integrated to the solution and kept under stirring for 1 hour until hydrolysis completion and polycondensation, following the protocol proposed by [10].

The microstructure and mechanical properties of materials obtained by sol-gel process depends on the hydrolysis and condensation reactions that are generally controlled by the solution's pH, due to the long time it takes for gelation with precursors used, some changes on pH were carried out to the proposed protocol in concordance with [17]. For that reason, the solution was adjusted to pH 8, 9 and 10 by addition of 5% NaOH solution to promote gelation. When a complete gelation of the solution was achieved, the gel was put on an oven at 70°C for 48 h for drying, to obtain the material powder, and finally washed until to eliminate salt.

2.3. Characterization of the bioactive glass

X-ray Diffraction (XRD) was used to obtain information of the crystal structure, chemical composition, and physical properties of the sample of the obtained bioactive glass. The assay was carried out using a Rigaku Miniflex X-ray powder diffractometer, equipped with a Cu source with λ = 1.5818 Å, ranging 2θ from 0° to 60° at 2°/min.

Raman Spectroscopy analysis was carried out to identify the characteristic wavelengths of obtained bioactive glass and check the correspondence of this material with bioactive glasses found in literature [18, 19]. The equipment used for this test was a RAMAN Spectometer (Dilor model LabRAM2), the test conditions were: Step beam from 0 to 3000 cm^{-1}, the wavelength used for this assay was 850 nm.

2.4. Production of CH/BG composite scaffolds

The CH/BG composite scaffolds were prepared using two different methods: adding to the chitosan solution either bioactive glass precursors BGi (*in situ*) or bioactive glass powder BGp, and different crosslinking agents (Poli vinil alcohol-PVA and Tripolyphosphate-TPP) to each of the resulting CH/BG solutions. Then, a subsequent freeze-drying process was carried out, to prepare the scaffolds and to obtain an adequate pore size and morphology. Crosslinking-free solutions were casted as control samples.

Production of in situ scaffolds CH/BGi

A solution of chitosan was previously prepared with a concentration of 2% w/v, dissolving chitosan commercial powder in a solution of 1% (v/v) acetic acid with magnetic stirring during 3 hours. Then, a solution containing TEOS/HNO$_3$, P$_2$O$_5$ and Ca(NO$_3$)$_2$.4H$_2$O as precursor compounds for bioactive glass production (*in situ*) was added to the chitosan solution.

The CH/BG precursor's solution was mixed thoroughly for 2 hours until fully homogenized. Crosslinking agent's solutions were prepared to be 1% wt and then added separately to beakers containing the CH/BGi solution. Then, these solutions were stirred for 15 minute, obtaining 3 different solutions: CH/BGi, CH/BGi/PVA and CH/BGi/TPP. Afterwards, the solution was put into sealed plastic containers and then frozen for 24 hours at -80 °C, for lyophilizing it for 24 hours.

Production of powder scaffolds CH/BGp

A solution of chitosan 2% (w/v) was prepared by dissolving chitosan powder in a solution 1% (v/v) acetic acid as before mentioned in the *in situ* protocol. After complete dissolution of the CH, BG powder (BGp), previously prepared, was added to the chitosan solution while the solution was still being stirred, for 2 more hours, until complete suspension of the BGp.

Crosslinking agent's solutions were prepared to be 1% wt and then added separately to beakers containing the CH/BGp solution and stirred for 15 min, obtaining 3 different solutions: CH/BGp, CH/BGp/PVA and CH/BGp/TPP. Then, the resulting solutions were then put under sonication for 30 minutes for degassing and then were transferred to plastic containers, frozen at -80 °C for 24 hours and lyophilized for 24 hours.

2.5. Characterization of the CH/BG scaffolds

The composite scaffolds were characterized by physicochemical and mechanical methods to test their potential as biomaterials.

Morphological characterization

The morphological characterization of the scaffold structure was carried out with Scanning Electron Microscopy (SEM) using a JEOL JSM 6490 LV microscope and the functional groups were obtained by Raman Spectroscopy using a Dilor LabraM2 spectrometer over a range of 500 to 3500 cm^{-1}.

Compression strength tests

Compression strength tests were carried out for scaffolds obtained in a regular universal machine DIGIMESS using a load distribution of 500 N and compression strain rate of 5 mm/min until deformation of 50%.

3. Results and discussion

3.1. X-Ray Diffraction of BG powder

XRD pattern of the BG samples is shown in Figure 1.

As is well known, glass is an amorphous material with no detectable diffraction maxima, therefore, when pH increases (pH=10), differences in crystallinity from this modification of the pH are observed.

The crystalline phases as some maxim diffraction can be observed are defined by the presence of diffraction peaks at 2θ = 23º, 29º, 32.5º, 35º, 39.8º, 42.7º, 48º and 55.5º corresponding to Na$_2$Ca$_2$Si$_3$O$_9$ phase of hexagonal system, because both the angular locations and the intensities of the sharp diffraction peaks match with those reported by [20].

The pH of solution seems to be an important factor setting the amorphous or crystalline character of the material after the thermal treatment, in concordance with [18, 21].
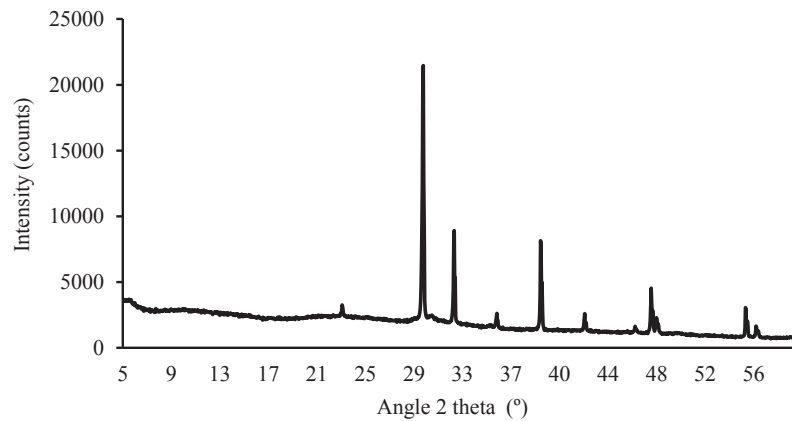
Figure 1 X-*Ray* diffraction pattern of bioactive glass powder
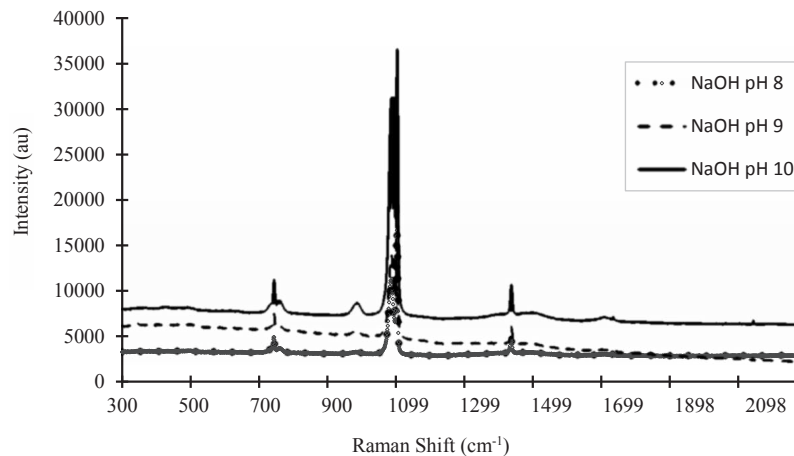
Figure 2 Raman spectrum of bioactive glass at different pH

3.2. Raman Spectroscopy of BG powder

Raman patterns of the studied samples are shown in Figure 2.

In Figure 2, four characteristic peaks of bioactive glasses are observed, one around 725 cm^{-1} (SiO$_4$), another to 1050 cm^{-1} corresponding to bond Si-O-Si, overlap with the peak at 1067 cm^{-1} (Si-O-Si), and other peak at 1400 cm^{-1} corresponding to bond Si-O-Si, which, compared to the literature, are around 100 cm^{-1} to the right of the spectrum. Taking this into account, they can relate these peaks with vibration bands of 58S bioactive glass [18, 19] and the bioglass with Na$^+$ addition presented by [22].

It is also notable that when pH increases in the process, are more remarkable peaks of bioactive glasses, and appears an additional low intensity peak near 950 cm^{-1}, which is related with bonds O-O. Besides that, only in samples treated with NaOH until pH 10, a peak at 1067 cm^{-1} is observed, which correspond to the presence of oxygen bridges (bridging oxygen's) and oxygen anti-bridge (non-bridging oxygen).

It is to notice that the pH has a remarkable effect on the crystallinity of the sample, because there is a rise in the intensity as the pH increases, which could be the cause of an improvement on the kinetic of the reaction, increasing the amount of Si-O and O-O bondages on the vitreous network. The electrical environment is changed due to the addition of NaOH, which changes the rheology of the system, increasing the viscosity (gelation).

The frequency shifting and intensity variations of the Raman bands observed for bioactive glasses are due to a decrease of the local symmetry originated by the addition of alkali to the silica network in concordance with [18, 23].

In particular, the samples at pH 10 have increased amounts of oxygen anti-bridge when pH increases, as well as increased oxygen bridge, confirming the theoretical assumption that there is a maximum condensation of silicates to basic pH, so it is probable that other molecules bioactive glass formulation proposals have actually joined silicates, thus promoting the formation of a stronger crystal lattice. The frequency shifting and intensity variations of the Raman bands observed for bioactive glasses are due to a decrease of the local symmetry originated by the addition of alkali to the silica network.

Well-defined vibrational bands characteristic of the Si–O–Si stretching and bending modes which are associated with the crystalline phases of the samples are observed either in concordance with [18].

3.3. Morphological Characterization of CH/BG scaffolds

Figures 3 to 5 show the SEM images for CH/BG *in situ* scaffolds (CH/BGi) and the PVA and TPP crosslinked scaffolds, denoted as CH/BGi/PVA and CH/BGi/TPP, respectively.

Interconnected pores are scarce in the observation plane, homogeneous distribution of the precursors of BG and typical CH sheet formation are observed. Also, a formation of radial channels is observable, consistent with the method of freezing and thermal gradient applied to the samples in the casting process. Possibly, channels or pores are formed in this direction, an example of this are the column-like pores seen in Figure 3.

CH/BGi composite scaffolds show abundant homogeneous pores with an adequate diameter, which provided a three-dimensional matrix with general porosity and high interconnection among the pores. These morphological characteristics are ideal for applications in tissue engineering because they allow the colonization of cells to assure a good integrity and functionality of the osteochondral construction.

The pores have a diameter ranging from 50-100 μm. In agreement with [24], the pores from 40-100 μm will allow the growth of blood vessels, which facilitate vascularization and bone mineralization. In this case, the scaffolds possess pores of the before mentioned dimensions; consequently, they could be used for bone reconstruction.

The presence of small pores smaller than 20 μm is also important for the protein absorption, ionic solubility, and the attachment of osteoblasts on the scaffolds [25]. This study revealed that CH/BGi scaffolds pores quite resemble a typical spongy 3D structure, with open pores, anisotropic porosity, and pore size ranging from 50 to 100 μm, as reported by [6, 10, 26, 27]. The surface morphology of the composite scaffold was rough because of the introduction of HA crystals in concordance with [28].

Samples containing PVA as crosslinking have interconnected pores, about 20-25 μm diameter, there is good distribution of the bioactive glass, with some clusters located. The same pattern observed in the BGi columns is also presented. The obtained pores are very close in size to those required for proper cell migration, as can be seen in Figure 4.

A similar porosity was observed on the TPP crosslinked scaffolds, in comparison to the PVA crosslinked ones, showing more defined edges and with a larger pore size (25-30 μm). A greater amount of BG was observed, with more particulate aggregates, more defined structures and thicker walls as seen in Figure 5.

The Figures 6 to 8 show the images obtained for scaffolds of CH and BG powder (CH/BGp) and the PVA (CH/BGp/PVA) and TPP (CH/BGp/TPP) crosslinked scaffolds, respectively.

Scaffolds casted with powder BG have a three-dimensional matrix with fewer pores (Figures 6, 7 and 8). It may be observed that the shape of BG is also different; the glass crystals have a rounded shape (Figure 6) and flat shape (Figure 8). Scaffolds with powder BG seem to have a denser structure, with a lower porosity, in comparison with other scaffolds.
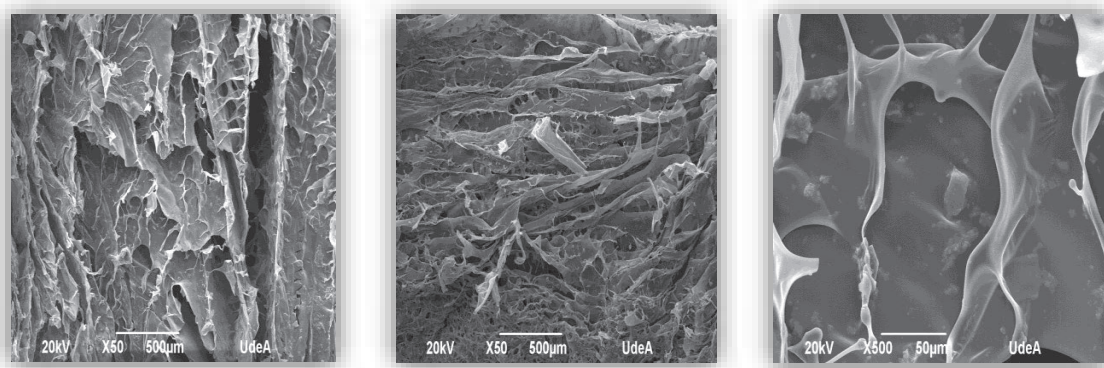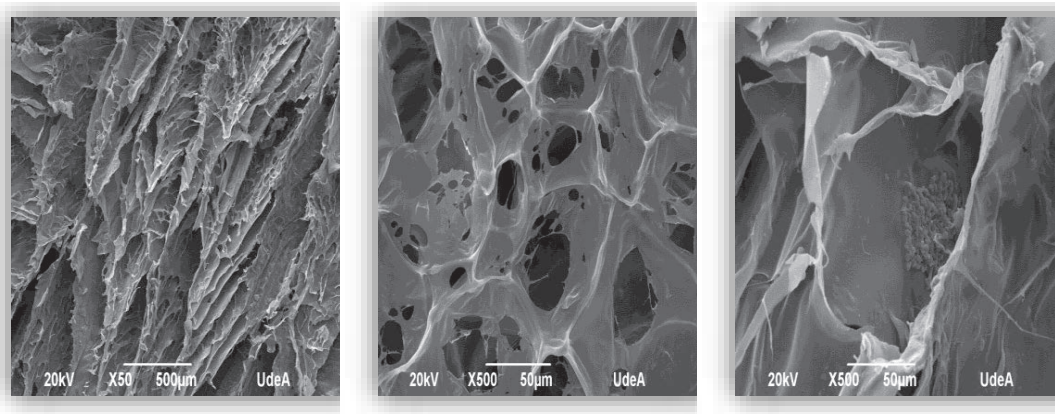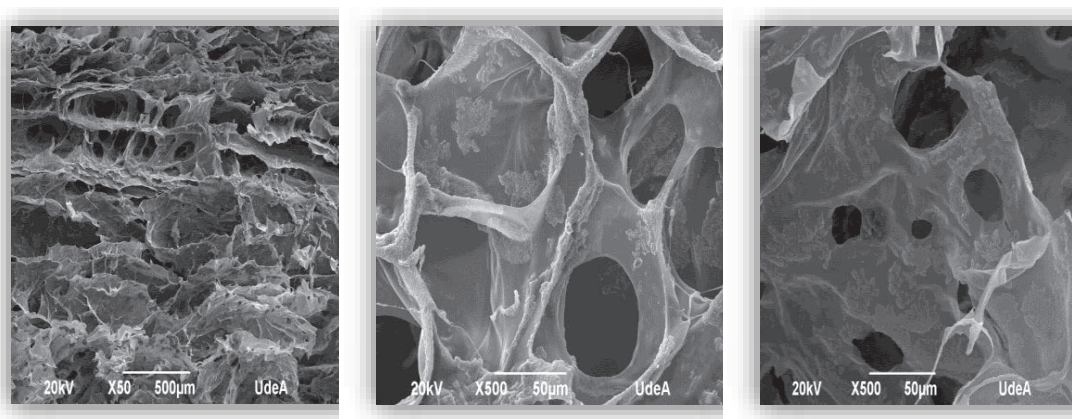

Figure 3 SEM micrographs of CH/BGi scaffold

Figure 4 SEM micrographs of CH/BGi/PVA scaffold

Figure 5 SEM micrographs of CH/BGi/TPP scaffold

The BGp scaffolds' structure is very different; these present pores, which are parallel to the direction of solidification. These pores are highly elongated, due to the precipitation of the particles of bioactive glass in the suspension. Those structures are similar to the presented by [14].

Scaffolds have a surface smoother than the previous ones and show a lower porosity. The bioactive glass particles are very well distributed and can easily distinguish two particle sizes, around 10 μm and smaller. This confirms the suspicion that the bioglass obtained by the sol-gel method produces microparticles of two different sizes. In the central image, a very good particle distribution and very low porosity is also observed.

A good distribution of BG powder on the surface of the scaffolds is also observed. Bioactive glass particles are crystals that seem to have a growth direction, given by the thermal gradient during the freezing process as well as by the maturing process of the BG. The homogeneous distribution of BG particles on the scaffold surface could generate more contact area for bone cells deposition, which is an advantage for biomineralization (Figure 6).

The particles morphology and distribution observed in the sample CH/BGp/PVA is similar to that seen on the CH/BGp

sample, except for the formation shown in the upper right side of Figure 7.

This formation is due solely to the use of PVA as crosslinking. Interconnected channels in the cross section (left) and low porosity in the outside (right) of the scaffold are also observed.

The CH/BGp/TPP sample has similar characteristics to the previous in the series. Its unique feature is the presence of more closed pores in the transversal face and a concentration of larger particles, probably due to inadequate homogenization of the particles provided by the fast action of the crosslinking on contact with the CH/BGp solution.

In general, the pore size in both kinds of scaffolds is controlled by the crosslinking agent. In concordance with [27, 29], it looks like on CH/Bgi samples, once BG nuclei were formed on the surface of chitosan scaffold, those could grow and spread out on the surface of scaffold with the increasing BG content.

CH and BG were homogenously combined through the *in situ* casting and the porous structure generated by the lyophilization showed good porosity and some cells could
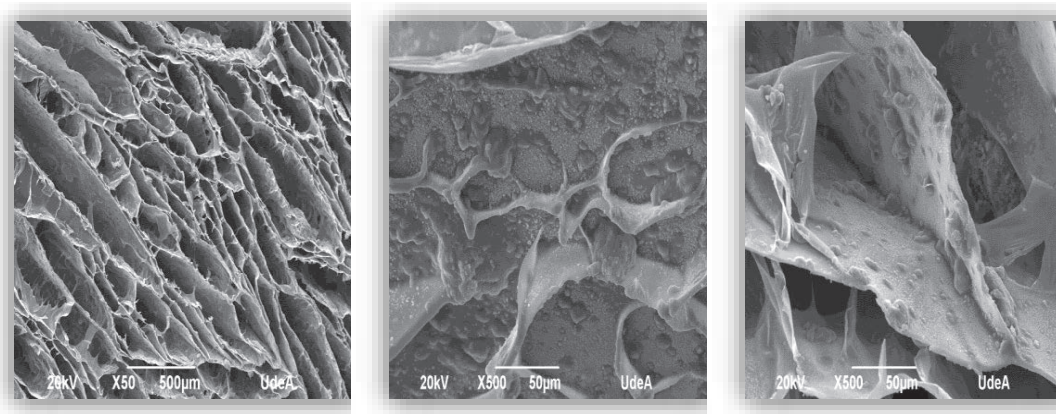
Figure 6 SEM micrographs of CH/BGp scaffold
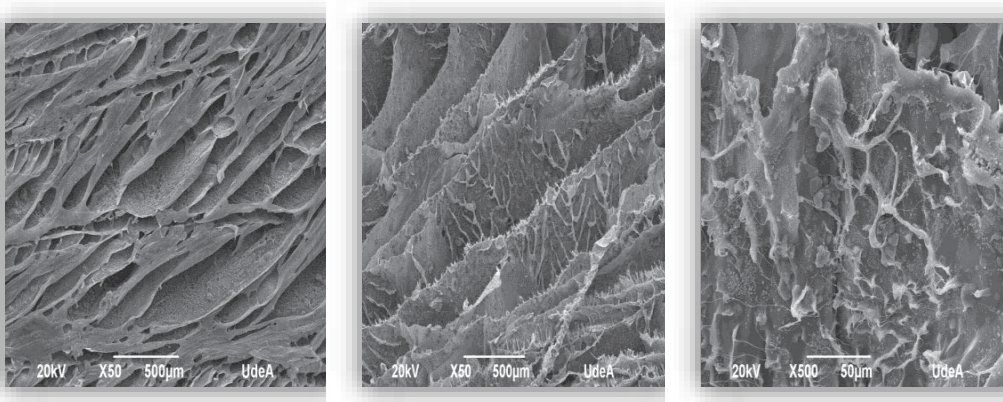
Figure 7 SEM micrographs of CH/BGp/PVA scaffold

grow in the pores of these 3-D scaffolds. Also, on scaffolds pore walls, the bioactive glass particles were inlaid in the chitosan surface like islands in concordance with reported by [30, 31].

3.4. Mechanical Characterization of the CH/BG scaffolds

In this section, the stress-strain (SS) plots for each of the samples are presented. Figure 9 shows the SS plot for the CH sample, which will be used as reference (Maximal stress (MS): 37.5 KPa) and the SS plots for CH/BGp (MS: 56.1 KPa) y CH/BGp/PVA (MS: 73.6 KPa) samples. It was not possible to obtain an adequate CH/BGp/TPP sample for mechanical characterization, due to a high crosslinking speed, which produced an amorphous and heterogeneous sample.

For the BGp series, a progressive improvement in the mechanical properties, in comparison with the reference, was observed. For the CH/BGp, mechanical resistance raised 33.15% and an additional 23.78% was gained by using PVA as crosslinking agent. A total improvement of 49.05% was obtained for the CH/BGp/PVA scaffold.

Figure 10 shows the SS plots for the BGi series, first CH/BGi (MS: 102.57 KPa), then CH/BGi/PVA (MS: 82.82 KPa) and finally, CH/BGi/TPP (MS: 47.56 KPa) samples.

In this series, the highest reinforcement was achieved for the CH/BGi sample (63.43%), while the CH/BGi/PVA (54.72%) and CH/BGi/TPP (21.15%) samples obtained a lower, not so significant improvement of the mechanical properties.

Comparing the effect of the BG's type (BGp or BGi) on the improvement of the scaffold's mechanical properties, it is clear that the reinforcement is more significant when BBG precursors are used instead of the BG powder, mainly due to a better, deeper interaction between BG precursors and CH when the solution is prepared and during lyophilization. Analyzing the effect of adding a crosslinking agent, PVA is clearly the best, showing the highest reinforcement for the CH/BGP series and achieving a good improvement of the mechanical properties in the CH/BGi series. The wave-like shape of the graphics shows a visco-elastic behavior of the scaffold (due to the chitosan) combining this with the collapsing of the pores of the porous structure of the CH/BG composite.
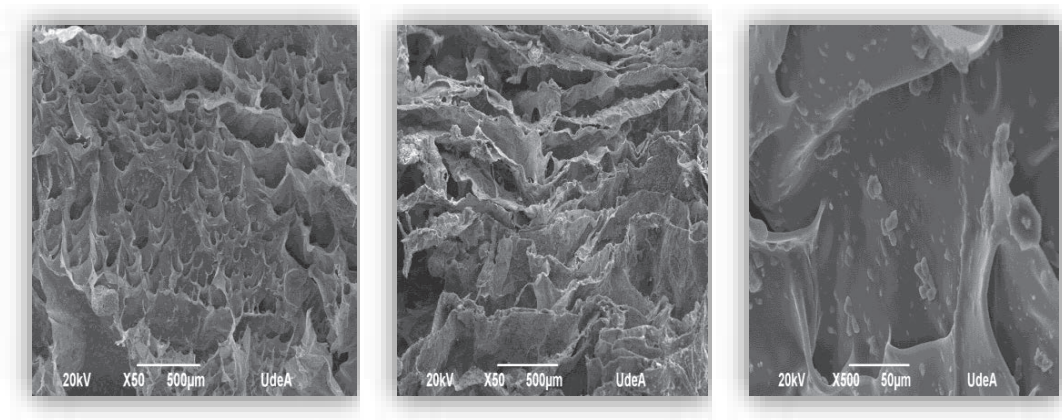
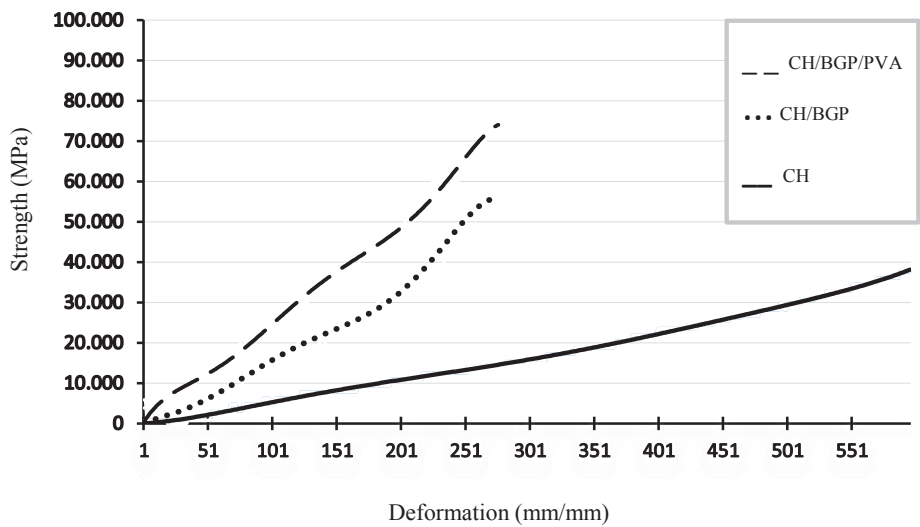**Figure 8** SEM micrographs of CH/BGp/TPP scaffold

Figure 9 SS plot for CH/BGp/PVA, CH/BGp and CH samples
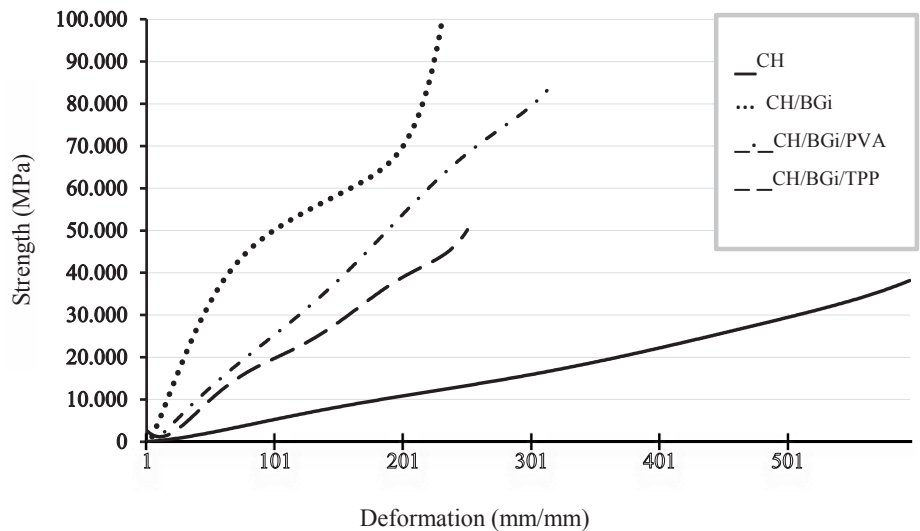

Figure 10 SS plot for CH, CH/BGi, CH/BGi/PVA and CH/BGi/TPP samples

4. Conclusions

The protocol proposed for the production of BG powder and the addition of NaOH, allows a reduction in gelation time, a more adequate size particle and a structure with higher crystallinity as the pH increases to 10, allowing it for use in tissue engineering scaffolds.

Scaffolds casted by the CH/BGi protocol have a 3D matrix with a highly porous microscopic structure and a high interconnection between the pores. Meanwhile, the BGp scaffolds have a 3D matrix with less porosity and smaller pores, showing that the CH/BGi scaffolds are good candidates for tissue engineering and bone regeneration.

This study has shown that desirable pore structure, mechanical properties and chemical composition of the composite scaffolds might be achieved through the control of the procedure and the ratio of BG, CH and crosslinking agents.

5. References

1. C. Estrada, A. Paz and L. López, "Ingeniería de tejido óseo: Consideraciones básicas", *Revista EIA- Escuela de Ingeniería de Antioquia*, vol. 5, pp. 93-100, 2006.
2. D. Balanta, "Utilización de quitosano procedente del micelio de Aspergillus Níger y su aplicación en regeneración de tejidos", M.S. thesis, Universidad del Valle, Cali, Colombia, 2014.
3. J. Jones, "Review of bioactive glass: From Hench to hybrids", *Acta Biomater.*, vol. 9, no. 1, pp. 4457-4486, 2013.
4. M. Mozafari and F. Moztarzadeh, "Synthesis, characterization and biocompatibility evaluation of sol-gel derived bioactive glass scaffolds prepared by freeze casting method", *Ceramics International*, vol. 40, no. 4, pp. 5349-5355, 2014.
5. L. Ramos, T. Montenegro and N. Pereira, "Perspectivas para o uso da quitosana na agricultura", *Revista Iberoamericana de Polímeros*, vol. 12, no. 4, pp. 195-215, 2011.
6. M. Alizadeh, F. Abbasi, A. Khoshfetrat and H. Ghaleh, "Microstructure and characteristic properties of gelatin/chitosan scaffold prepared by a combined freeze-drying/leaching method", *Materials Science and Engineering C*, vol. 33, no. 7, pp. 3958-3967, 2013.
7. H. Shibata, Y. Heo and S. Takeuchi, "Simple Molding Fabrication for Polyacrylamide Hydrogel", in *IEEE 24th International Conference on Micro Electro Mechanical Systems (MEMS)*, Cancun, Mexico, 2011, pp. 885-888.
8. J. Schwartz *et al.*, "Topical treatment of L. major infected BALB/c mice with a novel diselenide chitosan hydrogel formulation", *European Journal of Pharmaceutical Sciences*, vol. 62, pp. 309-316, 2014.
9. A. Paulino, J. Simionato, J. Garcia and J. Nozaki, "Characterization of chitosan and chitin produced from silkworm chrysalides", *Carbohydrate Polymers,* vol. 64, pp. 98-103, 2006.
10. M. Mozafari, M. Rabiee, M. Azami and S. Maleknia, "Biomimetic formation of apatite on the surface of porous gelatin/bioactive glass nanocomposite scaffolds", *Applied Surface Science*, vol. 257, no. 5, pp. 1740-1749, 2010.
11. F. Berthiaume, T. Maguire and M. Yarmush, "Tissue Engineering and Regenerative Medicine: History, Progress, and Challenges", *Annual Review of Chemical and Biomolecular Engineering*, vol. 2, pp. 403-430, 2011.
12. M. Rahaman *et al.*, "Bioactive glass in tissue engineering", *Acta Biomater.*, vol 7, no. 6, pp. 2355–2373, 2011.
13. B. Dorj, J. Park and H. Kim, "Robocasting chitosan/nanobioactive glass dual-pore structured scaffolds for bone engineering", *Materials Letters*, vol. 73, pp. 119-122, 2012.
14. P. Hunger, A. Donius and U. Wegst, "Structure-property-processing correlations in freeze-cast composite Scaffolds", *Acta Biomater.*, vol. 9, no. 5, pp. 6338-6348, 2013.
15. M. Peter et al., "Nanocomposite scaffolds of bioactive glass ceramic nanoparticles disseminated chitosan matrix for tissue engineering applications", *Carbohydrate Polymers*, vol. 79, no. 2, pp. 284-289, 2010.
16. C. Peniche, Y. Solís, N. Davidenko and R. García, "Chitosan/*hydroxyapatite-based composites*", *Biotecnol Apl.*, vol. 27, pp. 202-210, 2010.
17. C. Milea, C. Bogatu and A. Duta, "The influence of parameters in silica sol-gel process", *Bulletin of the Transilvania University of Brașov, Series I: Engineering Sciences*, vol. 4, no. 1, pp. 59-66, 2011.
18. A. Balamurugan *et al.*, "Synthesis and characterisation of sol gel derived bioactive glass for biomedical applications", *Materials Letters*, vol. 60, no. 29-30, pp. 3752-3757, 2006.
19. I. Notingher, A. Boccaccini, J. Jones, V. Maquet and L. Hench, "Application of Raman microspectroscopy to the characterisation of bioactive materials", *Materials Characterization*, vol. 49, no. 3, pp. 255-260, 2002.
20. J. Qian, Y. Kang, Z. Wei and W. Zhang, "Fabrication and characterization of biomorphic 45S5 bioglass scaffold from sugarcane", *Materials Science and Engineering: C*, vol. 29, no. 4, pp. 1361-1364, 2009.
21. G. Luz and J. Mano, "Preparation and characterization of bioactive glass nanoparticles prepared by sol-gel for biomedical applications", *Nanotechnology*, vol. 22, pp. 1-11, 2011.
22. D. Bellucci, G. Bolelli, V. Cannillo, A. Cattini and A. Sola, "*In situ* Raman spectroscopy investigation of bioactive glass reactivity: Simulated body fluid solution vs TRIS-buffered solution", *Materials characterization*, vol. 62, no. 10, pp. 1021-1028, 2011.
23. L. Marsich, L. Moimas, V. Sergo and C. Schmid, "Raman spectroscopic study of bioactive silica-based glasses: The role of the alkali/alkali earth ratio on the Non-Bridging Oxygen/Bridging Oxygen (NBO/BO) ratio", *Spectroscopy*, vol. 23, no. 3-4, pp. 227-232, 2009.
24. T. Wu *et al.*, "A new bone repair scaffold combined with chitosan/ hydroxyapatite and sustained releasing icariin", *Chinese Science Bulletin*, vol. 54, no. 17, pp. 2953-2961, 2009.
25. K. Zhang, D. Peschel, J. Helm, T. Groth and S. Fischer,

"FT Raman investigation of novel chitosan sulfates exhibiting osteogenic capacity, *Carbohydrate Polymers*, vol. 83, no. 1, pp. 60-65, 2011.

26. J. Oliveira *et al.*, "Novel hydroxyapatite/chitosan bilayered scaffold for osteochondral tissue-engineering applications: Scaffold design and its performance when seeded with goat bone marrow stromal cells", *Biomaterials*, vol. 27, no. 36, pp. 6123-6137, 2006.

27. S. Teng, E. Lee, P. Wang, S. Jun, C. Han and H. Kim, "Functionally Gradient Chitosan/Hydroxyapatite Composite Scaffolds for Controlled Drug Release", *Journal of Biomedical Materials Research Part B: Applied Biomaterials*, vol. 90B, no. 1, pp. 275-282, 2009.

28. K. Im *et al.*, "Organic-Inorganic hybrids of hydroxyapatite with chitosan", *Key Engineering Materials*, vol. 284-286, pp. 729-732, 2005.

29. H. Jin *et al.*, "In-situ formation of the hydroxyapatite/chitosan-alginate composite scaffolds", *Materials Letters*, vol. 62, no. 10-11, pp. 1630-1633, 2008.

30. L. Kong *et al.*, "Preparation and characterization of nano-hydroxyapatite/chitosan composite scaffolds", *Journal of Biomedical Materials Research Part A*, vol. 75, no. 2, pp. 275-282, 2005.

31. J. Weng and M. Wang, "Producing chitin scaffolds with controlled pore size and interconnectivity for tissue engineering", *Journal of Materials Science Letters*, vol. 20, no. 15, pp. 1401-1403, 2001.